Clinical Infectious Diseases

MAJOR ARTICLE

Epidemiology and Ecology of Severe Fever With Thrombocytopenia Syndrome in China, 2010–2018

Dong Miao,[1,a] Ming-Jin Liu,[2,a] Yi-Xing Wang,[1] Xiang Ren,[3] Qing-Bin Lu,[4] Guo-Ping Zhao,[1] Ke Dai,[1] Xin-Lou Li,[1] Hao Li,[1] Xiao-Ai Zhang,[1] Wen-Qiang Shi,[1] Li-Ping Wang,[3,b] Yang Yang,[2,b] Li-Qun Fang,[1,b] and Wei Liu[1,b]

[1]State Key Laboratory of Pathogen and Biosecurity, Beijing Institute of Microbiology and Epidemiology, Beijing, China, [2]Department of Biostatistics, College of Public Health and Health Professions, and Emerging Pathogens Institute, University of Florida, Gainesville, Florida, USA, [3]Division of Infectious Disease, Key Laboratory of Surveillance and Early-Warning on Infectious Diseases, Chinese Centre for Disease Control and Prevention, Beijing, China, and [4]School of Public Health, Peking University, Beijing, China

Background. The growing epidemics of severe fever with thrombocytopenia syndrome (SFTS), an emerging tick-borne disease in East Asia, and its high case fatality rate have raised serious public health concerns.

Methods. Surveillance data on laboratory-confirmed SFTS cases in China were collected. The spatiotemporal dynamics and epidemiological features were explored. The socioeconomic and environmental drivers were identified for SFTS diffusion using survival analysis and for SFTS persistence using a two-stage generalized boosted regression tree model.

Results. During 2010–2018, a total of 7721 laboratory-confirmed SFTS cases were reported in China, with an overall case fatality rate (CFR) of 10.5%. The average annual incidence increased >20 times and endemic areas expanded from 27 to 1574 townships, whereas the CFR declined from 19% to 10% during this period. Four geographical clusters—the Changbai Mountain area, the Jiaodong Peninsula, the Taishan Mountain area, and the Huaiyangshan Mountain area—were identified. Diffusion and persistence of the disease were both driven by elevation, high coverages of woods, crops, and shrubs, and the vicinity of habitats of migratory birds but had different meteorological drivers. Residents ≥60 years old in rural areas with crop fields and tea farms were at increased risk to SFTS.

Conclusions. Surveillance of SFTS and intervention programs need to be targeted at areas ecologically suitability for vector ticks and in the vicinity of migratory birds to curb the growing epidemic.

Keywords. SFTS; epidemiology; ecology; diffusion; modeling.

Severe fever with thrombocytopenia syndrome (SFTS) is an emerging tick-borne infectious disease with a wide clinical spectrum, ranging from mild febrile illness accompanied by thrombocytopenia and/or leukocytopenia to severe hemorrhagic fever, clinical encephalitis, and multiple organ failure, with a case fatality rate (CFR) of 12–50% [1–3]. The etiological pathogen is a novel phlebovirus (SFTS virus [SFTSV]) in the family *Phenuiviridae* of the order *Bunyavirales* [1]. The disease was identified first in China in 2010 and subsequently in South Korea and Japan in 2013 [1, 4, 5]. The cumulative numbers of cases were 5360 (lab-confirmed) in China by 2016, 866 in South Korea by 2018, and 467 in Japan by August 2019, according to the most recent updates [6–8]. Recently, Vietnam also reported 2 new cases [9]. SFTSV is genetically closely related to Heartland virus, a novel phlebovirus first isolated from 2 famers in the United States in 2009, and the 2 viruses cause similar clinical symptoms including acute fever and thrombocytopenia [10]. Despite the high CFR and rapid spread of SFTS, no vaccine or antiviral specifically targeting SFTSV are available for the time being.

The public health concern of SFTSV is primarily posed by the wide distribution of its vectors and the broad spectrum of its animal hosts [1]. *Haemaphysalis longicornis*, which is thought to be the primary vector of SFTSV, is widely distributed in East Asia, Australia, New Zealand, and Hawaii and has recently invaded the mainland of the United States [11], possibly via transportation of livestock and seasonal migration of birds [11, 12]. Environmental changes, particularly those in climate and landscape, may have fueled the spatial expansion of ticks, raising serious concerns about potentially growing epidemics of SFTSV and other tick-borne pathogens across continents [13, 14]. Meanwhile, the epidemiological features and ecological niches of SFTS remain elusive.

In the current study, we provide a broad and in-depth epidemiological analysis of the SFTS epidemics in China using the

Received 27 January 2020; editorial decision 20 May 2020; published online 17 October 2020.

[a]D. M. and M. -J. L. contributed equally to this work.

[b]These senior authors, L.-P. Wang, Y. Yang, L.-Q. Fang, and W. Liu, equally contributed as co-corresponding authors.

Correspondence: W. Liu, State Key Laboratory of Pathogen and Biosecurity, Beijing Institute of Microbiology and Epidemiology, 20 Dong-Da St, Fengtai District, Beijing, China 100071 (liuwei@bmi.ac.cn).

Clinical Infectious Diseases® 2021;73(11):e3851–8

DOI: 10.1093/cid/ciaa1561

most updated surveillance data, focusing on spatiotemporal patterns of the disease and socioeconomic and environmental risk drivers for its diffusion and persistence. This study aims not only to bridge knowledge gaps in epidemiology and ecology of the disease but also to provide a risk assessment approach for planning surveillance and control of SFTS in countries where either the disease or the associated vector ticks are emerging.

METHODS

Data Sources

De-identified individual-level epidemiological data of SFTS patients during 2010–2018 were extracted from the China Information System for Disease Control and Prevention (CISDCP). The death data were further supplemented by a prospective study conducted in Xinyang, Henan Province [3]. County-level demographic and socioeconomic data were obtained from the National Bureau of Statistics of China. County-level and township-level land cover data of China surveyed in 2005 and 2015 were downloaded (http://www.geodata.cn). Transportation routes were obtained from the digital maps of China at the scale of 1:100 000 as previously described [15]. Monthly meteorological data during 2010–2018 were obtained from the China Meteorological Data Sharing Service System (http://cdc.nmic.cn/home.do) and transformed into 19 ecoclimatic indexes (Supplementary Table 1) [16]. Multicollinearity among the ecoclimatic indexes was screened by pairwise Pearson correlation coefficients. Highly correlated predictors were grouped using the package "NbClust" (https://cran.r-project.org/web/packages/NbClust/index.html) provided in the statistical software R (R Core Team, 2013), and only 1 predictor from each group was used for subsequent analyses (Supplementary Material and Methods). The ecoclimatic indexes were grouped at the township level (Supplementary Table 2) and the county levels (Supplementary Table 3) separately. The location data of 4 tick species carrying SFTSV, *H. longicornis*, *Diptera silvarum*, *Rhipicephalus microplus,* and *Isoetes sinensis*, were derived from our previous studies. Risk categories (1 = high, 0 = low) for the presence of the 4 tick species were calculated from statistical models and serve as potential risk factors for subsequent ecological modeling of SFTS (Supplementary Material and Methods). For simplicity in description, we refer to the high- and low-risk categories as presence and absence of the tick species, respectively.

The Spatial Diffusion of SFTS and Associated Risk Determinants

The location of each lab-confirmed case was georeferenced based on the residential address at the township level. Geographical clusters of SFTS cases were identified by a spatial trend surface analysis [17]. For each identified cluster, we used joinpoint regression to explore the temporal trend of annual disease incidences and a radar chart of standardized monthly incidences to display seasonality [18, 19]. Cox proportional hazards models in the R software package "survival" (https://cran.r-project.org/web/packages/survival/index.html) were applied to explore potential risk factors (Supplementary Table 4) driving the disease diffusion at the township level. Cox proportional hazards models were also fitted to each cluster separately to explore spatial heterogeneity in risk drivers.

Ecological Modeling and Risk Prediction for SFTS

We employed a 2-stage generalized boosted regression tree (GBRT) model in the R software package "Xgboost" (https://cran.r-project.org/web/packages/xgboost/index.html) to explore potential factors (Supplementary Table 5) contributing to the presence or incidence of SFTS and to predict the risks of the disease at the county level in mainland China [20]. At the first stage, a logistic structure was used to fit the presence/absence of SFTS cases by county and year, which accounted for the excessive amount of zero case numbers in the majority of the nation. At the second stage, a gamma distribution was fitted to the nonzero annual incidences. Details about screening of multicollinearity, cross-validation for tuning parameters, and assessment of goodness-of-fit were given in the Supplementary Materials and Methods.

RESULTS

From 2010 to 2018, a total of 11 995 SFTS patients in 25 provinces were reported, of whom 7721 (64.4 %) were laboratory confirmed. Among the confirmed patients, 810 died, leading to a case fatality rate of 10.5% (95% confidence interval [CI]: 9.8–11.2%) (Table 1). The median age was 63 years (interquartile range [IQR]: 54–70 years), and slightly more cases were female (52.6%). The median age increased from 56 years in 2010 to 64 years in 2018 (Supplementary Figure 1), probably reflecting the natural aging of the at-risk population and the lack of replenishment of the exposed population. Gender distribution was similar between years but differed across months, with higher proportions of female patients hospitalized in April (64%) and May (60%) than in other months (49%) ($P < .001$). Median time from disease onset to hospitalization was 8 days (IQR: 4–9 days) in 2010, decreased to 7 days in 2011, and flattened at 6 days (IQR: 4–9 days) in the subsequent years. The CFR declined from 19% in 2010 to 10% in 2018 (trend test $P < .001$). Both decreased in the time to hospitalization, and CFR were likely due to improved diagnosis and increased awareness of the disease in endemic regions. CFRs in the epidemic months (April–August) were higher than those off the season ($P = .004$), although hospital admission delay did not differ between months.

Spatial Clustering of SFTS Cases

The trend surface analysis identified 4 distinct geographical clusters, where 94.7% of all confirmed cases in China were reported (Figure 1). Cluster I is located at the Changbai Mountain

Table 1. Baseline Demographic Characteristics of Laboratory-confirmed SFTS Patients in China from 2010 to 2018, for the Whole Nation and Stratified by Cluster

	Total	Cluster I	Cluster II	Cluster III	Cluster IV	Other
No. of confirmed cases	7721	386	1510	1128	4286	411
Annual incidence (/10^5)	0.064	0.099	0.92	0.16	0.20	0.0048
Average annual percent change (95% CI)	18.5 (3.5, 35.6)	14 (2.3, 27)	18.9 (10, 28.5)	31.6 (27, 36.4)	11.2 (−4.5, 29.4)	25.1 (10.2, 42.2)
No. of deaths	810	20	185	107	450	48
Case fatality ratio % (95% CI)	10.5 (9.8, 11.2)	5.2 (3.3, 8)	12.3 (10.7, 14)	9.5 (7.9, 11.4)	10.5 (9.6, 11.5)	11.7 (8.8, 15.3)
Age in years median (IQR)	63 (54–70)	62 (55–70)	64 (55–71)	63 (55–71)	62 (52–70)	65 (55–73)
No. (%) of female cases	4063 (52.6)	165 (42.7)	730 (48.3)	567 (50.3)	2383 (55.6)	218 (53)
Days from disease onset to admission, median (IQR)	6 (4–9)	6 (3–9)	6 (4–9)	6 (4–8)	6 (4–9)	5 (2–8)
Seasonality	May–August	July–September	May–August	May–August	April–July	May–August

Abbreviations: CI, confidence interval; IQR, interquartile range.

area in Liaoning Province of northeastern China. Two clusters reside in Shandong province on the northern part of the east coast, cluster II on the Jiaodong Peninsula, and cluster III surrounding the Taishan Mountain area. Cluster IV, the largest among the 4 clusters, centers around the Huaiyangshan Mountain area in central China and stretches over 5 provinces: Henan, Anhui, Hubei, Jiangsu, and Zhejiang. These 4 endemic foci are situated in 4 different ecogeographical zones but share similar mountainous or hilly landscapes covered by forests, shrubs, or grassland and temperate humid or subtropical weathers (Supplementary Figure 2). The highest average annual incidence, 0.92 per 10^5 persons, was observed in cluster II, followed by 0.20, 0.16, and 0.10 per 10^5 in clusters IV, III, and I, respectively. The age and gender profiles showed disparity across clusters (Table 1).

Temporal Trend and Seasonality

At the national level, the annual incidence increased steadily from 0.0041/10^5 in 2010 to 0.098/10^5 in 2015, peaked in 2016 at 0.1/10^5, and started to drop after 2017 (Figure 1A). The national temporal trend was dominated by that in cluster IV where both the case number and population size outweigh the other 3 clusters (Figure 1E). The average annual percent change (AAPC) in cluster IV decreased from 37.7% during 2010–2015 to −22.1% thereafter, marking a sharp turnaround (Figure 2E). In contrast, clusters I–III clearly displayed an increasing trend over the surveillance years (Figure 1B–D). Particularly, the persistent increasing trend in cluster III with an AAPC of 31.6% warrants close surveillance in this region.

Similar trends were observed in the total area of affected townships, increasing from 2010 to the peak in 2016 and dropped slightly after 2017 (Figure 2F). The growth of the affected areas in clusters I, II, and III was much slower than that of the annual incidences, but the growth became somewhat faster after 2016 in clusters I and III (Figure 2G–I). The temporal pattern in cluster IV resembled that of the nation but with a quicker drop after 2016 (Figure 2J).

The SFTS epidemics at the national level were highly seasonal. The epidemic season spanned from May to August with a peak in May (Figure 2K–O). For individual clusters, the epidemic season appeared to be slightly later at a higher latitude, for example, July–September in cluster I (40°N) versus April–July in cluster IV (30°N), and the peak months occurred in July, June, May in clusters I, II, and IV, respectively. Cluster III had 2 peaks, one in May and the other in August.

Spatial Diffusion and Driving Factors of SFTS

Multiple endemic foci of SFTS had been established as early as 2011, and the disease mainly spread from the center of each cluster to its surrounding areas (Supplementary Figure 3). The periodicity in the baseline hazards of reporting the first SFTS case at the township level further confirmed the strong seasonality of SFTSV (Supplementary Figure 4). The spread was fueled by high levels of elevation and seasonal variation of precipitation with hazard ratios (HR) of 2.04 (95% CI: 1.87–2.24) and 1.79 (95% CI: 1.57–2.05), respectively (Supplementary Table 6). On the contrary, a high coverage of rural settlement, a long distance to the nearest freeway/highway, and a long distance to the nearest habitat of migratory birds impeded the disease diffusion (Supplementary Table 6 and Supplementary Figure 5). The estimated effects of influential predictors were mostly consistent with the diffusion trend when overlaid on the maps, including elevation, land cover, and distance to the nearest habitat of migratory birds (Figure 3). For example, the diffusion of the disease from high to low elevations was clear in clusters I, II, and IV (Figure 3A, D, and G). Survival analyses revealed similar effects for elevation, coverage of rainfed cropland, and distance to the nearest wetland across the 4 clusters (Supplementary Table 7 and Supplementary Figure 6*B*), However, there also appears to be heterogeneity in some effects across the clusters. For example, the hazard increased linearly with a longer distance to the nearest freeway/highway in cluster II (Supplementary Table 7), but the association was opposite in cluster IV (Supplementary Figure 6*D*). In

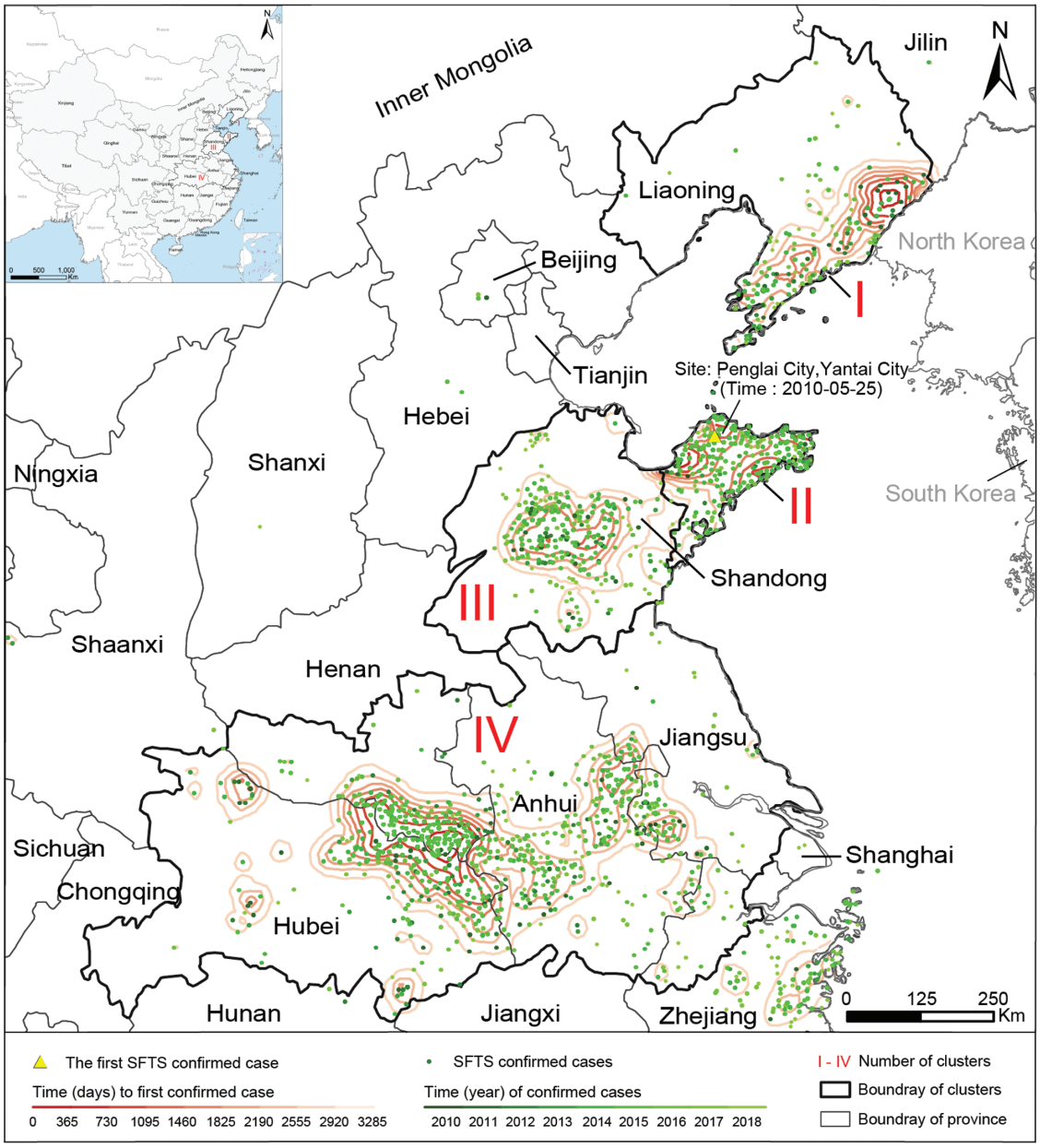

Figure 1. Spatial dispersion of 4 geographic clusters of SFTS cases in China, 2010–2018. Confirmed SFTS cases were marked as dots with the color indicating the year of reporting. Four clusters (I–IV) were delineated according to the spatial trend surface analysis and the geographic aggregation of cases. In each cluster, contour lines of the time intervals (in days) from the first case reported in China to the first case reported in each SFTS-affected township reflect the diffusion direction of the disease. Abbreviation: SFTS, severe fever with thrombocytopenia syndrome.

addition, a longer distance to the nearest habitat of migratory birds was associated with a lower hazard in cluster I and IV, a higher hazard in cluster III, and a nonlinear trend in cluster II (Supplementary Table 7 and Supplementary Figure 6C).

Distribution of and Drivers for the Ecological Risk of SFTS

According to the 2-stage GBRT models, altitude, the coverage of closed-canopy woodland, proportion of senior residents (≥60 years old), and precipitation in the driest season were important drivers (RC ≥5%) for the presence of SFTS cases (Supplementary Table 8). Among the counties with reported SFTS cases, the coverage of tea farms was the leading factor contributing to higher incidences, with an RC of nearly 14%. Other important factors include population density, the proportion of senior residents, gross domestic product (GDP), the number of hospitals, and the coverages of rainfed cropland, closed-canopy woodland, and shrubland. Two factors, the proportion of senior residents and the coverage of closed-canopy woodland, contributed RCs >5% for both stages of the model.

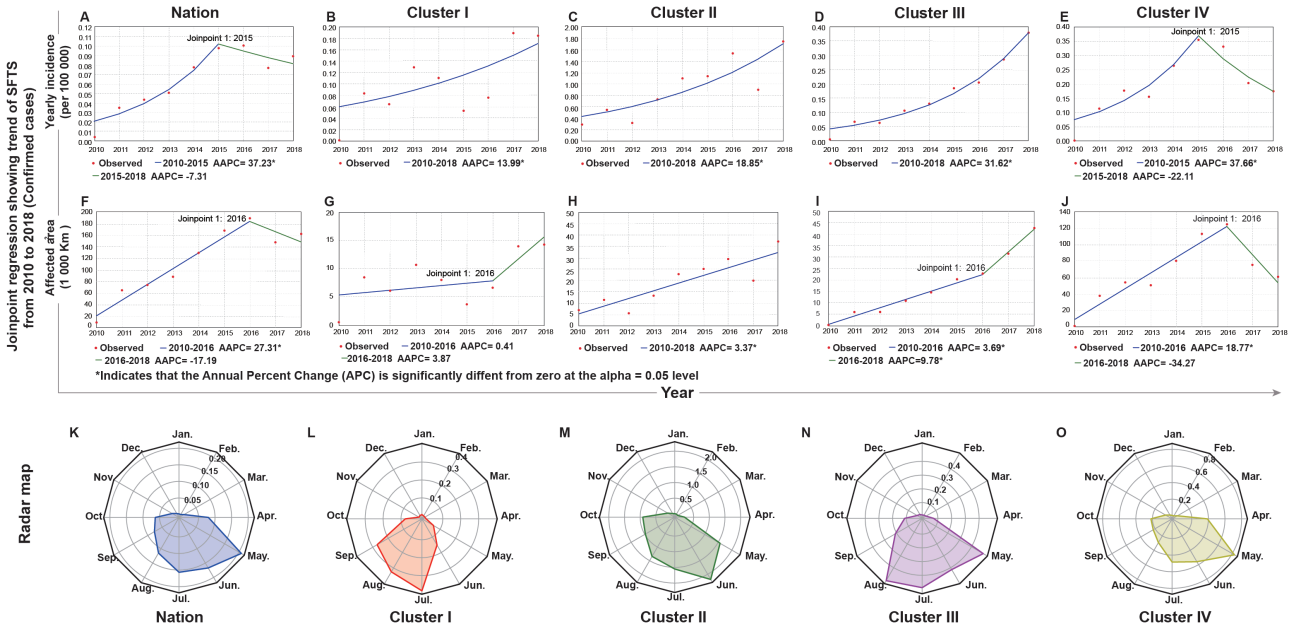

Figure 2. Temporal trend and seasonality of SFTS epidemics in China from 2010 to 2018. Blue solid lines indicate the trends in the annual incidence of confirmed cases and in total areas of affected townships for the nation (*A* and *F*) and the 4 geographic clusters (*B–E* and *G–J*) fitted by joinpoint regression. Lines change color from blue to green if a joinpoint is identified. AAPCs were estimated based on the slopes of the lines. Red dots indicate observed incidence. Panels *K–O* indicate seasonal pattern of confirmed SFTS patients in the nation and clusters I–IV, respectively. Seasonality is presented as a radar diagram. Circumference is divided into 12 months in a clockwise direction, and the radius represents average monthly incidences over 2010–2018. Abbreviations: AAPC, average annual percentage changes; SFTS, severe fever with thrombocytopenia syndrome.

The presence of *H. longicornis* contributed moderately to the presence of SFTS (RC = 3.68). The lower-than-expected contribution is possibly due to the inclusion of social-environmental variables that were predictive for and thus correlated with the presence of the tick vector. The exact associations of model-predicted incidence with 10 factors with RC ≥5%, as well as the annual average temperature and the presence of *H. longicornis*, are shown in Supplementary Figures 7–9. The model successfully differentiated low-risk from high-risk counties, although the predictability is less impressive for the moderate-risk group (Supplementary Table 9). The overall predictive performance was satisfactory with AUCs of 99% and 96% for the training and testing datasets, respectively (Supplementary Table 10). The spatial distribution of model-predicted incidences largely matched that of the observed incidences in the endemic regions, with extra ecologically suitable high-risk areas predicted, mostly in the vicinity of the observed high-incidence areas where no cases have been reported yet (Supplementary Figure 10).

DISCUSSION

By synthesizing surveillance, socioeconomic and environmental data during 2010–2018 in mainland China, we provided an up-to-date and in-depth overview of the epidemiological and ecological characteristics of SFTS. Four distinct geographic clusters were identified, among which epidemiological characteristics and diffusion patterns are comparable but also with important differences. Cluster IV, where cases earlier than 2010 were retrospectively found [21], had the highest disease burden but showed a sign of declining incidence since 2016. In contrast, the other 3 clusters, particularly cluster III, are still seeing increasing disease incidence, calling for more active preventive and control programs.

Via diffusion analyses and ecological modeling, we found that altitude and coverages of woodland, rainfed cropland, and shrubland were highly influential for both diffusion and persistence of the disease. Although disease diffusion was faster at higher altitudes, disease incidence was actually higher at lower altitudes (≤300m), likely a consequence of diffusion from high to low altitudes. These environmental conditions are directly related to the ecological suitability of the vector ticks as well as animal hosts [2]. *H. longicornis*, a major vector of SFTVS, is widely distributed in China with habitats found in most provinces [22]. *H. longicornis* has been adapted to a broad range of ecological conditions but is most active and reproductive where vertebrates are abundant and climate is moist and warm [23]. The preferred ecological environment by *H. longicornis* were common in regions with low and middle altitudes, high coverage of woodland, rainfed cropland, and shrubland. The geographic expansion of *H. longicornis* in the recent decades has drawn wide attention and was possibly driven by climatic and environmental changes [24]. The direct account of variables

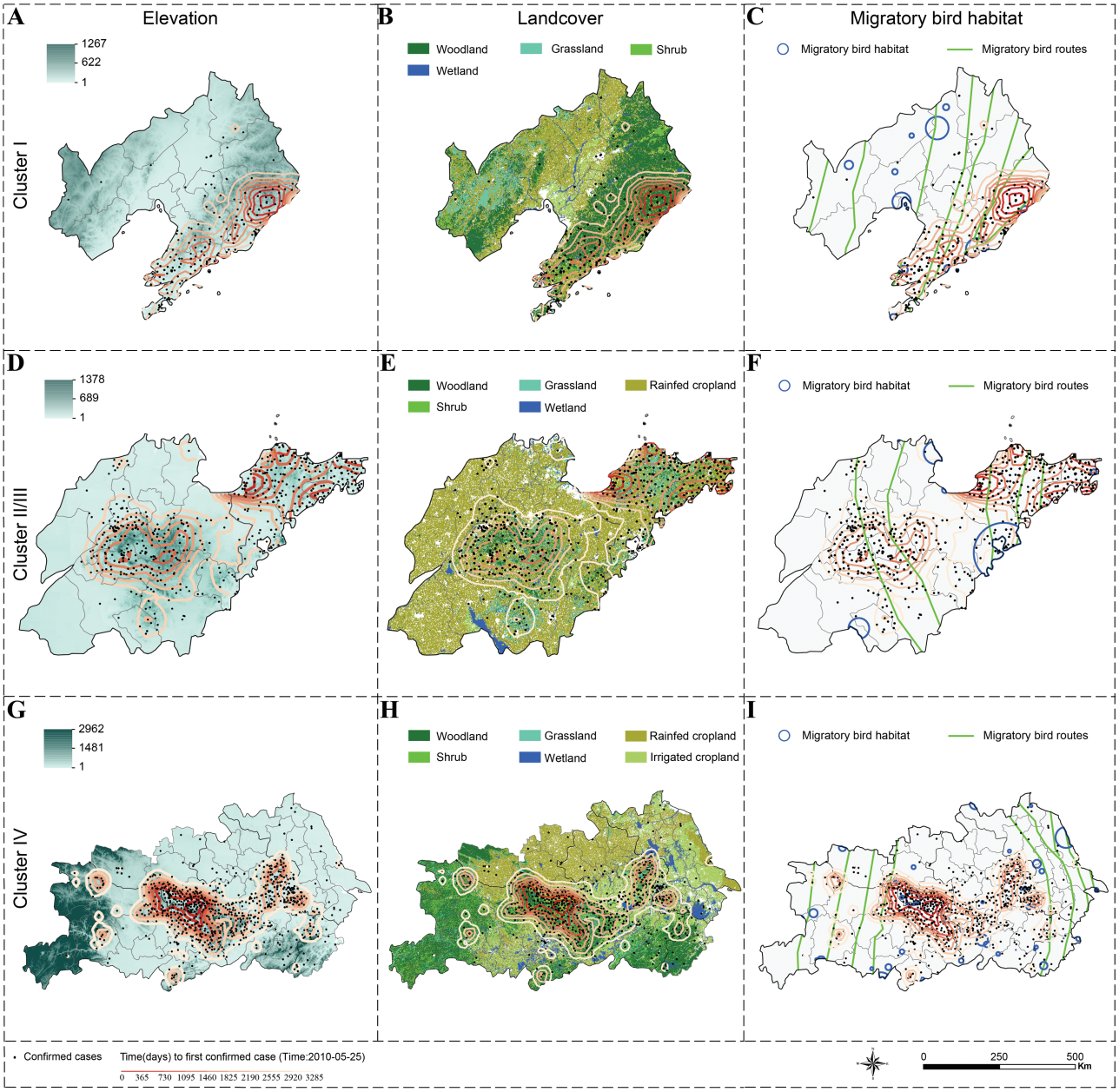

Figure 3. Association between spatial diffusion and influential factors identified by the Cox proportional hazards model by geographic cluster. Spatial diffusion is represented by the trend surface contour plots with darker color indicating earlier importation time of the first case in the township. Columns correspond to the influential factors: elevation (*A, D, G*), land cover (*B, E, H*), and distance to the nearest migratory bird habitat (*C, F, I*); rows are arranged according to geographic clusters: cluster I (*A–C*), clusters II and III (*D–F*), and cluster IV (*G–I*).

that are indicative of ecological suitability for *H. longicornis* explains why the vector itself is only moderately influential in our ecological model for SFTS.

We also found that a high coverage of rural settlement and a long distance to habitats of migratory birds could protect against both diffusion and incidence of SFTS, although the effect was moderate for the incidence. Rural settlement refers to man-made constructions in rural areas, with coverage inversely proportional to the coverage of crop fields and wooded areas, and therefore a negative association is expected. The negative association of disease diffusion with the distance to habitats of migratory birds is also not surprising, given numerous studies reporting evidence for transportation of ticks via migrating birds [13, 25–27]. For example, the expansion of *Amblyomma maculatum* from southeastern states towards northern and western states during the past few decades in the United States was thought to be partly due to immature ticks carried by migratory birds along the Atlantic flyway [25]. *H. longicornis*

was found on a variety of migratory birds including *Zoothera aurea*, *Turdus hortulorum*, *Halcyon coromanda*, *Pitta nympha*, and *Anas platyrhynchos*, which were found in eastern or northeastern China [13, 28, 29]. Antibodies against SFTSV were detected migratory birds such as *Anser cygnoides* and *Streptopelia chinensis* in eastern China [14]. We used the A4 category in the Directory of Important Bird Areas (IBA) in China (mainland): Key Sites for Conservation by Bird Life International (2009) to represent habitats of migratory birds [30]. This category of IBAs comprises of sites that, on a regular or predictable basis, hold congregations of either ≥1% of the global population of ≥1 species, or ≥20 000 water birds, or migratory species exceeding thresholds at bottleneck sites. In contrast to the negative association in other clusters, a longer distance to habitats of migratory birds appears to imply a higher risk in cluster III. However, cluster III is the only cluster where its center is about 100 kilometers away from the nearest habitat (Figure 3), suggesting this counterintuitive effect could be artificial.

The associations of SFTS incidence with low levels of population density, GDP and number of hospitals are consistent with the fact that the majority of patients were rural residents. The percentage of residents ≥60 years old was a driving factor for both presence and high incidence of SFTS. In rural areas of the endemic regions, young adults pursue work opportunities in urban cities most of the year, and the senior adults become the majority of the exposed population through agricultural activities. Similarly, women assume more tea-farming activities than men, which may partly account for the higher SFTS incidence among females in April–June, the tea-harvesting season. This is also consistent with the strong influence of coverage of tea farms on SFTS incidence.

Compared to our previous ecological modeling for the presence of SFTS using the surveillance data during 2010–2013 [31], the current analysis modeled both presence/absence and the magnitude of incidence. The inclusion of more data and screening for multicollinearity further improved the robustness of statistical inference about ecological drivers and predictive power for disease risks. Other countries with existing or emerging establishment of *H. longicornis*, such as South Korea, Japan, and the United States, can use this model to assess potential risks of SFTS and to target surveillance and control measures at high-risk regions [32–34].

Our study is subjected to a few limitations. The CFRs might be underestimated as some patients with adverse clinical progression were discharged per family's request for economic reasons [3]. Therefore, we did not pursue further death-related analysis. In addition, the diffusion analysis did not consider the possibility that the first detection of SFTS cases in some places could be due to improved diagnosis rather than recent disease spread. Finally, our ecological model was built on annual incidence at the county level. The relatively large space and time units may subject our analyses to ecological fallacy [35].

In summary, our study presented key epidemiological characteristics and ecological drivers of the emerging SFTS epidemics in China. The drivers for diffusion and persistence of the disease are mostly related to the ecological suitability of the competent vector of SFTSV, *H. longicornis*. The ongoing growth of the disease burden is likely associated with the geographic expansion of the vector possibly via transportation of livestock and migratory birds, analogous to the observation that this vector emerged and spread quickly in North America. Meanwhile, we recommend active surveillance of SFTSV and *H. longicornis* be placed in countries and regions with ecological suitability for the tick vector, especially those trading livestock with or on the flyway of migratory birds from East Asia. The highly predictive ecological model developed in the current study can be used to assess the risk levels of SFTS in agricultural or wooded areas where the disease has not been reported.

Supplementary Data

Supplementary materials are available at *Clinical Infectious Diseases* online. Consisting of data provided by the authors to benefit the reader, the posted materials are not copyedited and are the sole responsibility of the authors, so questions or comments should be addressed to the corresponding author.

Notes

Author contributions. W. L., L.-Q. F., and Y. Y. designed the study. L.-P. W., Q.-B. L., K. D., H. L., and X.-A. Z. performed data sorting and database establishment. D. M., M.-J. L., and Y.-X. W. conducted the analyses under supervision of W. L., L.-Q. F., and Y. Y., and L.-P. W., G.-P. Z., X.-L. L., and W.-Q. S. helped with the analyses. Y. Y., L.-Q. F., and W. L. wrote the draft of the manuscript. L.-P. W. and X. R. collected the SFTS surveillance data. All authors contributed to and approved the final version of the manuscript.

Acknowledgments. The authors thank all medical personnel contributing to the ascertainment and reporting of human SFTS cases in China.

Financial support. This study was supported by the China Mega-Project for Infectious Diseases (grant 2018ZX10201001, 2018ZX10713002, 2018ZX10101003), and National Natural Science Foundation of China (grant 81825019). Y. Y. was supported by the US National Institutes of Health R01 (grant numbers AI139761 and AI116770).

Potential conflicts of interest. The authors: No reported conflicts of interest. All authors have submitted the ICMJE Form for Disclosure of Potential Conflicts of Interest.

References

1. Yu XJ, Liang MF, Zhang SY, et al. Fever with thrombocytopenia associated with a novel bunyavirus in China. N Engl J Med **2011**; 364:1523–32.
2. Liu Q, He B, Huang SY, Wei F, Zhu XQ. Severe fever with thrombocytopenia syndrome, an emerging tick-borne zoonosis. Lancet Infect Dis **2014**; 14:763–72.
3. Li H, Lu QB, Xing B, et al. Epidemiological and clinical features of laboratory-diagnosed severe fever with thrombocytopenia syndrome in China, 2011–17: a prospective observational study. Lancet Infect Dis **2018**; 18:1127–37.
4. Kim KH, Yi J, Kim G, et al. Severe fever with thrombocytopenia syndrome, South Korea, 2012. Emerg Infect Dis **2013**; 19:1892–4.
5. Takahashi T, Maeda K, Suzuki T, et al. The first identification and retrospective study of severe fever with thrombocytopenia syndrome in Japan. J Infect Dis **2014**; 209:816–27.
6. Sun J, Lu L, Wu H, Yang J, Ren J, Liu Q. The changing epidemiological characteristics of severe fever with thrombocytopenia syndrome in China, 2011–2016. Sci Rep **2017**; 7:9236.
7. Korea Center for Prevention and Control of diseases. Surveillance data on infectious diseases in Korea. Available at: https://www.cdc.go.kr/npt/biz/npp/ist/bass/bassAreaStatsMain.do#. Accessed 25 September 2019.

8. Japanese National Institute of Infectious Diseases. Investigation and surveillance of SFTS patients in Japan. Available at: https://www.niid.go.jp/niid/ja/id/2245-disease-based/sa/sfts/idsc/idwr-sokuhou/7415-sfts-nesid.html. Accessed 25 September 2019.
9. Tran XC, Yun Y, Van An L, et al. Endemic severe fever with thrombocytopenia syndrome, Vietnam. Emerg Infect Dis **2019**; 25:1029–31.
10. McMullan LK, Folk SM, Kelly AJ, et al. A new phlebovirus associated with severe febrile illness in Missouri. N Engl J Med **2012**; 367:834–41.
11. Rainey T, Occi JL, Robbins RG, Egizi A. Discovery of *Haemaphysalis longicornis* (Ixodida: Ixodidae) parasitizing a sheep in New Jersey, United States. J Med Entomol **2018**; 55:757–9.
12. United States Department of Agriculture. National *Haemaphysalis longicornis* (longhorned tick) Situation Report. Available at: https://usdasearch.usda.gov. Accessed 29 August 2018.
13. Yun Y, Heo ST, Kim G, et al. Phylogenetic analysis of severe fever with thrombocytopenia syndrome virus in South Korea and migratory bird routes between China, South Korea, and Japan. Am J Trop Med Hyg **2015**; 93:468–74.
14. Li Z, Bao C, Hu J, et al. Ecology of the tick-borne phlebovirus causing severe fever with thrombocytopenia syndrome in an endemic area of China. PLoS Negl Trop Dis **2016**; 10:e0004574.
15. Fang LQ, de Vlas SJ, Liang S, et al. Environmental factors contributing to the spread of H5N1 avian influenza in mainland China. PLoS One **2008**; 3:e2268.
16. Hijmans RJ, Cameron SE, Parra JL, et al. Very high resolution interpolated climate surfaces for global land areas. Int J Climatol **2010**; 25:1965–78.
17. Fang LQ, Yang Y, Jiang JF, et al. Transmission dynamics of Ebola virus disease and intervention effectiveness in Sierra Leone. Proc Natl Acad Sci U S A **2016**; 113:4488–93.
18. Kim HJ, Fay MP, Feuer EJ, Midthune DN. Permutation tests for joinpoint regression with applications to cancer rates. Stat Med **2000**; 19:335–51.
19. Saary MJ. Radar plots: a useful way for presenting multivariate health care data. J Clin Epidemiol **2008**; 61:311–7.
20. Chen T, Guestrin T. "XGBoost: a scalable tree boosting system," 22nd SIGKDD Conference on Knowledge Discovery and Data Mining, **2016**, https://arxiv.org/abs/1603.02754.
21. Bao CJ, Guo XL, Qi X, et al. A family cluster of infections by a newly recognized Bunyavirus in eastern China, 2007: further evidence of person-to-person transmission. Clin Infect Dis **2011**; 53:1208–14. doi:10.1093/cid/cir732.
22. Chen Z, Yang X, Bu F, Yang X, Yang X, Liu J. Ticks (acari: ixodoidea: argasidae, ixodidae) of China. Exp Appl Acarol **2010**; 51:393–404.
23. Heath A. Biology, ecology and distribution of the tick, *Haemaphysalis longicornis* Neumann (Acari: Ixodidae) in New Zealand. N Z Vet J **2016**; 64:10–20.
24. Tufts DM, VanAcker MC, Fernandez MP, DeNicola A, Egizi A, Diuk-Wasser MA. Distribution, host-seeking phenology, and host and habitat associations of *Haemaphysalis longicornis* ticks, Staten Island, New York, USA. Emerg Infect Dis **2019**; 25:792–6.
25. Sonenshine DE. Range expansion of tick disease vectors in North America: implications for spread of tick-borne disease. Int J Environ Res Public Health **2018**; 15:478.
26. Lindeborg M, Barboutis C, Ehrenborg C, et al. Migratory birds, ticks, and Crimean-Congo hemorrhagic fever virus. Emerg Infect Dis **2012**; 18:2095–7.
27. Elfving K, Olsen B, Bergström S, et al. Dissemination of spotted fever rickettsia agents in Europe by migrating birds. PLoS One **2010**; 5:e8572.
28. Heath ACG, Palma RL, Cane RP, Hardwick S. Checklist of New Zealand ticks (Acari: Ixodidae, Argasidae). Zootaxa **2011**; 2995:55–63. doi:10.5281/zenodo.203775.
29. Kang T Kang YM, Jeong W, Moon OK, et al. Spring migration of mallards (*Anas platyrhynchos*) tracked with wild-trackers in East Asia. J Asia-Pacific Biodiversity **2016**; 9:323–7.
30. China Bird Watching Network. **2009**. Available at: http://www.chinabirdnet.org/iba_inventory.html. Accessed 25 August 2019.
31. Liu K, Cui N, Fang LQ, et al. Epidemiologic features and environmental risk factors of severe fever with thrombocytopenia syndrome, Xinyang, China. PLoS Negl Trop Dis **2014**; 8:e2820.
32. Hoogstraal H, Roberts FH, Kohls GM, Tipton VJ. Review of *Haemaphysalis* (Kaiseriana) *longicornis* Neumann (resurrected) of Australia, New Zealand, New Caledonia, Fiji, Japan, Korea, and Northeastern China and USSR, and its parthenogenetic and bisexual populations (Ixodoidea, Ixodidae). J Parasitol **1968**; 54:1197–213.
33. Rochlin I. Modeling the Asian longhorned tick (Acari: Ixodidae) suitable habitat in North America. J Med Entomol **2019**; 56:384–91.
34. Raghavan RK, Barker SC, Cobos ME, et al. Potential spatial distribution of the newly introduced long-horned tick, *Haemaphysalis longicornis* in North America. Sci Rep **2019**; 9:498.
35. Wakefield J. Ecologic studies revisited. Annu Rev Public Health **2008**; 29:75–90.